Applied research on the diagnostic value of ^{18}F-FDG PET/CT in different subtypes mantle cell lymphoma

Yixuan Ren[1,2] **MD,**
Jiamin Chen[1] **MD,**
Chao Wang[2] **MD,**
Xiaozhu Lin[2] **MD,**
Shu Cheng[2] **MD,**
Xufeng Jiang[1,2] **MD,**
Dongxu Chen[1] **MD**

1. Department of Nuclear Medicine, Wuxi Xinwu District Xinrui Hospital, Wuxi, Jiangsu, China.
2. Department of Nuclear Medicine, Ruijin Hospital, Shanghai Jiao Tong University School of Medicine, Shanghai 200025, China

Keywords: Mantle cell lymphoma (MCL) - ^{18}F-FDG PET/CT - Aggressive variants

Corresponding author:
Dongxu Chen,
Wuxi Xinwu District Xinrui Hospital, 197 Zhixian Road, Wuxi 214000, Jiangsu, China
Tel:+86-14780408526
2796372336@qq.com);
Xufeng Jiang,
Ruijin Hospital, 197 Ruijin 2nd Road, Shanghai 200025, China
Tel:+86-18916760377
jxf10885@rjh.com.cn

Received:
3 October 2024
Accepted revised:
5 March 2025

Abstract

Objective: To analyze the diagnostic value of fluorine-18-fluoro-deoxyglucose positron emission tomography/computed tomography (^{18}F-FDG PET/CT) in mantle cell lymphoma (MCL) and explore its application in distinguishing between the classic and aggressive variants of MCL. **Subjects and Methods:** Retrospective analysis was performed on the ^{18}F-FDG PET/CT imaging, clinical, and pathological data of 134 newly diagnosed MCL patients confirmed by pathology. **Results:** Among the 134 patients, 97.8% had increased ^{18}F-FDG uptake in lymph nodes, and 88.8% had increased ^{18}F-FDG uptake in extranodal tissues or organs. In the diagnosis of bone marrow infiltration in MCL patients, ^{18}F-FDG PET/CT has demonstrated a high specificity rate of 86.4% and a limited sensitivity rate of 43.9%. Fluorine-18-FDG PET/CT performs well in diagnosing gastric and intestinal infiltration, with high accuracies of 85.0% and 91.7% respectively. The receiver operating characteristic (ROC) curve analysis revealed that a diagnostic threshold of maximum standardized uptake value (SUVmax) at 10.4 effectively distinguished between the classic and aggressive variants of MCL, achieving a sensitivity of 68.0%, a specificity of 80.7%, and an accuracy of 79.1%, with an area under the curve (AUC) value of 0.771. **Conclusion:** Fluorine-18-FDG PET/CT has a high positive detection rate in both intra-nodal and extra-nodal lesions of MCL at initial diagnosis. It exhibits high specificity and positive predictive value (PPV) in diagnosing bone marrow infiltration and possesses strong comprehensive diagnostic capabilities in gastrointestinal infiltration. Furthermore, the SUVmax can be used to distinguish between the classic and aggressive variants of MCL, and it is significantly positively correlated with the Ki-67 index, providing valuable clinical reference.

Hell J Nucl Med 2025; 28(1): 36-43 *Epub ahead of print: 7 April 2025* *Published online: 30 April 2025*

Introduction

Mantle cell lymphoma (MCL) is a rare and incurable aggressive subtype of B-cell non-Hodgkin lymphoma (NHL), accounting for approximately 6%-8% of all NHL cases [1]. It predominantly affects middle-aged and elderly individuals, with a median age at diagnosis of 60 years. The incidence rate is significantly higher in males than in females, with a male-to-female ratio of approximately 2-4:1 [2]. Mantle cell lymphoma is characterized by poor prognosis, with a median survival duration of only 3-5 years [3]. Clinically and biologically, MCL exhibits a high degree of heterogeneity, with approximately 10%-20% of patients manifesting an indolent course, while others may present with aggressive lymphoma [4, 5]. Based on the size of nucleus, chromatin pattern, and mitotic activity, MCL can be classified into classic and aggressive variants, with the latter accounting for 10%-20% of MCL cases [6]. The aggressive variants include blastoid and pleomorphic subtypes, which are often resistant to conventional therapies, resulting in difficulties in achieving durable remission [7, 8]. Accurate subtype classification is significance for the treatment and management of MCL, as it involves understanding a spectrum of molecular and pathological features. This task requires the expertise of a specialized pathologist.

Fluorine-18-fluoro-deoxyglucose (^{18}F-FDG) positron emission tomography/computed tomography (PET/CT) has extensive applications in lymphoma assessment [9], but significant variations exist among different pathological types of lymphoma in PET/CT imaging. Current research on MCL primarily focuses on staging [10-13]. Compared to computed tomography (CT), ^{18}F-FDG PET/CT is able to detect more lesions, leading to an upstaging of the disease [14]. In the study by Albano et al. (2019) [10], 122 patients with MCL were staged, and the results showed that PET/CT altered the staging and treatment plans of 23 patients, among which two patients avoided unnecessary invasive treatment,

while 21 patients were upstaged to an advanced stage and underwent more aggressive chemotherapy. A systematic review analyzed 209 MCL patients from 25 studies and found that ^{18}F-FDG PET/CT altered the staging of 41 patients (19.6%), with 36 patients (17.2%) being upstaged due to the detection of additional extranodal lesions on PET/CT [11].

The prognostic value of ^{18}F-FDG PET/CT in MCL is another area of focus [15, 16]. These findings suggest that metabolic parameters of ^{18}F-FDG PET/CT, such as SUVmax, metabolic tumor volume (MTV) and total lesion glycolysis (TLG) can effectively determine the progression free survival and overall survival of MCL patients.

In studies concerning the staging and prognosis of MCL, the determination of positivity is primarily based on visual assessment or semi-quantitative parameters as the criteria, rather than pathological diagnosis. We all know that ^{18}F-FDG is not MCL-specific imaging agent, so the positive lesions are not necessarily MCL infiltration. However, few studies reported the diagnostic performance of ^{18}F-FDG PET/CT in MCL compared with pathology. The possible reason is that MCL may involve multiple organs at the same time, and it is difficult to biopsy different lesions in clinical work. In addition, MCL is rare, and it is difficult to have sufficient data for evaluation.

This retrospective study analyzed the ^{18}F-FDG PET/CT images and clinicopathological data of 134 newly diagnosed MCL patients, aiming to explore the imaging characteristics and diagnostic performance of MCL on ^{18}F-FDG PET/CT. Furthermore, we compared the differences in ^{18}F-FDG PET/CT and clinicopathological features between classic and aggressive variants of MCL, providing a reference for clinical applications.

Subjects and Methods

Patients

This study retrospectively analyzed MCL patients who underwent ^{18}F-FDG PET/CT examination at our hospital, from January 2018 to April 2024. The pathological diagnostic criteria for MCL were based on the WHO Classification of Tumours of Haematopoietic and Lymphoid Tissues (2016) [17]. Patients were excluded if they had no clear pathological data, had chemotherapy before the ^{18}F-FDG PET/CT, had a history of other malignancies, or had a fasting blood glucose level ≥11.1mmol/L before the examination.

A total of 134 patients with MCL were enrolled in our study, comprising 109 males (81.3%) and 25 females (18.7%), with male patients approximately 4.3 times the number of females. The median age at onset was 62.5±9.2 years, ranging from 37 to 85 years. Notably, prior to the PET/CT examination, 10 patients underwent resection of affected organs or lesions for diagnostic or therapeutic purposes, resulting in the non-visualization of these lesions on ^{18}F-FDG PET/CT images. These excluded lesions encompassed 3 spleens, 2 orbital tumors, 2 segments of the intestine, 2 parotid glands, and 1 unilateral testicle, which were not included in our statistical analysis. All patients were pathologically confirmed with MCL, including 109 cases of the classic subtype, 22 cases of the blastoid variant, and 3 cases of the pleomorphic variant.

Since lymphoma patients often have multiple lesions simultaneously, pathological examination is the only gold standard to determine these lesions. However, it is an invasive procedure, and we cannot perform pathological biopsy on all lesions. In this study, pathological diagnosis of 1-6 sites was performed in each patient, with a total of 292 sites (multiple lymph nodes were counted as 1 site). Table 1 lists the basic information of the included population and the sites of lesions that were confirmed through pathological biopsy.

Table 1. *Patients' characteristics.*

Characteristics	Number (%)		
Age/years	62.5±9.2		
Male/Female	109/25		
Cellular morphological variants			
Classic subtype	109 (81.3%)		
Blastoid variant	22 (16.4%)		
Pleomorphic variant	3 (2.2%)		
Ann-Arbor (Cotswolds revised) stage			
I-II	15 (11.2%)		
III-IV	119 (88.8%)		
The site of histopathological diagnosis			
Site	**Number (%)**	**Diagnosis**	
		MCL	**Not MCL**
Total	292	228	64
Lymph node	98 (33.6%)	98	0
Bone marrow	112 (38.4%)	57	55
Intestine	24 (8.2%)	21	3
Waldeyer's ring	21 (7.2%)	20	1
Stomach	20 (6.8%)	15	5
Spleen	6 (2.1%)	6	0
Parotid gland	5 (1.7%)	5	0
Orbital tumors	3 (1.0%)	3	0
Nasal cavity	2 (0.7%)	2	0
Unilateral testicle	1 (0.3%)	1	0

Note: lesions that underwent resection were not included.

^{18}F-FDG PET/CT examination

Fluorine-18-FDG was produced by the Tracerlab FXF-N (GE Healthcare, USA) synthesis system with a radiochemical purity of >95%. The PET/CT scanning instrument used was the Discovery VCT 64 (GE Healthcare, USA). All patients were instructed to fast for at least 6 hours prior to the procedure. ^{18}F-FDG was administered intravenously at a dose of 3.70 to 5.55MBq/kg, followed by a 60-minute wait in a quiet state before performing the whole-body PET/CT scan. The scanning range extended from the top of the head to the upper one-third of the femur, with a total of 6 to 7 bed positions. For the CT scan, a tube voltage of 140kV and a tube current of 120 to 180mAs were used, with a slice thickness of 3.75mm. Computed tomography data were used for attenuation correction, and images were reconstructed using an iterative method to obtain transverse, sagittal, and coronal CT, PET, and PET/CT fusion images.

^{18}F-FDG PET/CT interpretation

The images were jointly reviewed by two experienced nuclear medicine physicians, and any differences in opinion were resolved through mutual consultation. The staging criteria were in accordance with the Ann-Arbor (Cotswolds revised) staging system [18]. The largest lymph node was chosen, and its short diameter was measured; it was considered positive if its SUVmax was greater than that of the mediastinal blood pool. Increased metabolism in bone marrow and spleen was considered positive when SUVmax was greater than that of the liver, while for other locations, visual assessment was based on the background surrounding the lesion tissue [19, 20].

Statistical analysis

Statistical analysis was performed using SPSS 23.0 (SPSS Statistics, IBM, USA). Quantitative data were tested for normality, with normally distributed data expressed as mean± standard deviation (x±s) and non-normally distributed data presented as Min-Max. The single sample T-test was used to compare the SUVmax of pathologically diagnosed lesions with the lesions identified as positive by PET/CT. Mann-Whitney U tests for non-normally distributed data, and Chi-squared tests or Fisher's exact test for comparisons of proportions. Pearson correlation analysis was employed for correlation analysis. The diagnostic threshold of SUVmax was determined by plotting the receiver operating characteristic (ROC) curve. A P-value of less than 0.05 was considered statistically significant.

Results

The characteristics of MCL on ^{18}F-FDG PET/CT

All 134 patients exhibited pathological ^{18}F-FDG uptake on ^{18}F-FDG PET/CT. Among them, 131 patients (97.8%) had increased 18F-FDG uptake in lymph nodes, and 119 patients (88.8%) had abnormally increased ^{18}F-FDG uptake in extranodal tissues or organs. The spleen, Waldeyer's ring, bone marrow and gastrointestinal tract are the most commonly involved extranodal sites of MCL. Different anatomical sites exhibit varying degrees of ^{18}F-FDG uptake, with relatively lower SUVmax in bone marrow and spleen. Table 2 presents the proportion of positive lesions in different sites and their SUVmax values.

Since not all ^{18}F-FDG PET/CT positive lesions were biopsied, we compared the differences in SUVmax between pathologically diagnosed lesions and those diagnosed only by ^{18}F-FDG PET/CT in Table 3. The results showed that the SUVmax of ^{18}F-FDG PET/CT positive lesions in bone marrow was higher than the SUVmax of pathologically confirmed bone marrow infiltration. There was no significant difference in lymph nodes, Waldeyer's ring, stomach and intestine.

^{18}F-FDG PET/CT in MCL bone marrow and gastrointestinal infiltration

In this study, a cohort of 112 patients underwent bone marrow aspiration biopsy, whereas 24 patients underwent colonoscopy, and 20 patients received gastroscopic biopsy prior to undergoing systemic treatment. Among these patients, 57 cases (50.9%) were definitively diagnosed with bone marrow infiltration, 21 cases (87.5%) exhibited intestinal infiltration, and 15 cases (75.0%) were diagnosed with gastric infiltration. Fluorine-18-FDG PET/CT has high specificity (86.4%) in the diagnosis of bone marrow infiltration, but its sensitivity is relatively low (43.9%), with an accuracy of 67.9%. Fluorine-18-FDG PET/CT performs well in diagnosing gastric and intestinal infiltration, with high accuracies of 85.0% and 91.7% respectively. Table 4 presents a comparison of the diagnostic capabilities of ^{18}F-FDG PET/CT versus pathological outcomes in detecting MCL infiltration in bone marrow and the gastrointestinal tract.

^{18}F-FDG PET/CT distinguishing the morphological variants of MCL

This study analyzed the differences between the classic and aggressive variants of MCL in terms of ^{18}F-FDG PET/CT and clinical features. The results indicated that both the Ki-67 index and SUVmax of the aggressive variant were significantly higher than those of the classic variant, with statistical significance. As detailed in Table 5.

The ROC curve analysis indicated that the diagnostic threshold of SUVmax for distinguishing the classic and aggressive variants of MCL was 10.4, with an AUC value of 0.771. When SUVmax was greater than 10.4, the diagnosis was made as the aggressive variant, and otherwise, it was classified as the classic type. The sensitivity was 68.0%, the specificity was 80.7%, and the accuracy was 79.1%. Additionally, we analyzed the correlation between the Ki-67 index and SUVmax, and the results showed a moderate correlation between the two (r=0.400, P=0.000). The ROC curve is presented in Figure 1.

Discussion

Fluorine-18-FDG PET/CT can reflect the glucose metabolic

Table 2. *MCL positive lesion distribution and SUVmax in ^{18}F-FDG PET/CT.*

Site	Number	%[a]	SUVmax
Lymph node	131	97.8	8.2±5.3
Spleen	67	50.0	5.7±3.1
Waldeyer's ring	63	47.0	9.4±3.7
Bone marrow	32	23.9	4.9±2.0
Intestine	39	29.1	9.8±5.0
Stomach	33	24.6	7.2±3.2
Skin	11	8.2	7.7±2.3
Thyroid	9	7.5	2.9-16.8
Parotid gland	4	3.0	3.0-10.3
Nasal cavity	2	1.5	8.10-38.50
Pleura	2	1.5	3.0-3.1
Scrotum	2	1.5	3.79-15.70
Prostate	2	1.5	6.0-10.2
Kidney	2	1.5	4.9-5.2
Breast	1	0.7	7.0
Eyelid	1	0.7	6.7
Lung	1	0.7	3.4
Pancreas	1	0.7	3.1
Gall bladder	1	0.7	8.0

Note: a. the ratio of patients with positive lesions at the specific site to the total number of patients.

Table 3. *Comparison of SUVmax values between pathologically diagnosed lesions and ^{18}F-FDG PET/CT positive lesions.*

Site	Pathologically confirmed		PET/CT positive		t	P value
	Number/n	SUVmax	Number/n	SUVmax		
Lymph node	98	8.3±5.0	131	8.2±5.3	0.261	0.794
Waldeyer's ring	21	8.9±4.5	63	9.4±3.7	-0.461	0.650
Bone marrow	57	3.5±1.9	32	4.9±2.0	-5.452	＜0.001
Stomach	15	8.1±4.4	33	7.2±3.2	0.818	0.427
Intestine	21	9.1±6.2	39	9.8±5.0	-0.492	0.628

Table 4. *MCL positive results in ^{18}F-FDG PET compared with pathological diagnosis.*

Site	Number	PET results	Pathologic diagnosis		Sensitivity	Specificity	PPV[a]	NPV[b]	Accuracy
			MCL	Other					
Bone marrow	112	Positive (29)	25	4	43.9%	86.4%	86.2%	61.4%	67.9%
		Negative (83)	32	51					
Stomach	20	Positive (16)	14	2	93.3%	60.0%	87.5%	75.0%	85.0%
		Negative (4)	1	3					
Intestine	24	Positive (19)	19	0	90.5%	100%	100%	60.0%	91.7%
		Negative (5)	2	3					

Note: a. positive predictive value (PPV); b. negative prediction value (NPV)

Table 5. *Comparison of differences between typical and aggressive MCL variants in ^{18}F-FDG PET/CT and clinical features.*

Characteristics	Classical type	Aggressive variant	t/χ^2	P
Number	109 (81.3%)	25 (18.7%)	-	-
Age/year	63.2±8.9	59.5±10.1	1.810	0.073
Ki-67	29.8±15.1	78.0±19.4	-13.590	0.000
SUVmax	8.4±4.7	14.5±8.2	-3.548	0.001
Minor axis of the largest lymph node	2.2±1.4	2.5±1.3	-0.794	0.429
Proportion of III-IV stages	96(88.1%)	23(92.0%)	0.044	0.834
Proportion extranodal infiltration	99(92.5%)	25(100%)	1.328	0.249
Proportion of bone marrow Infiltration[a]	44(49.4%)	13(56.5%)	0.367	0.545
Proportion of increased bone Marrow metabolism	22(20.2%)	10(40.0%)	4.393	0.036
Proportion of splenomegaly	56(52.3%)	15(62.5%)	0.816	0.366
Proportion of increased spleen Metabolism[b]	51(47.7%)	16(66.7%)	2.833	0.092
Proportion of increased Gastrointestinal metabolism	46(42.2%)	7(28.0%)	1.716	0.190

Note: a Only 112 patients who underwent bone marrow biopsy were included in the statistics. b The 3 patients who underwent splenectomy were not included in the statistics.

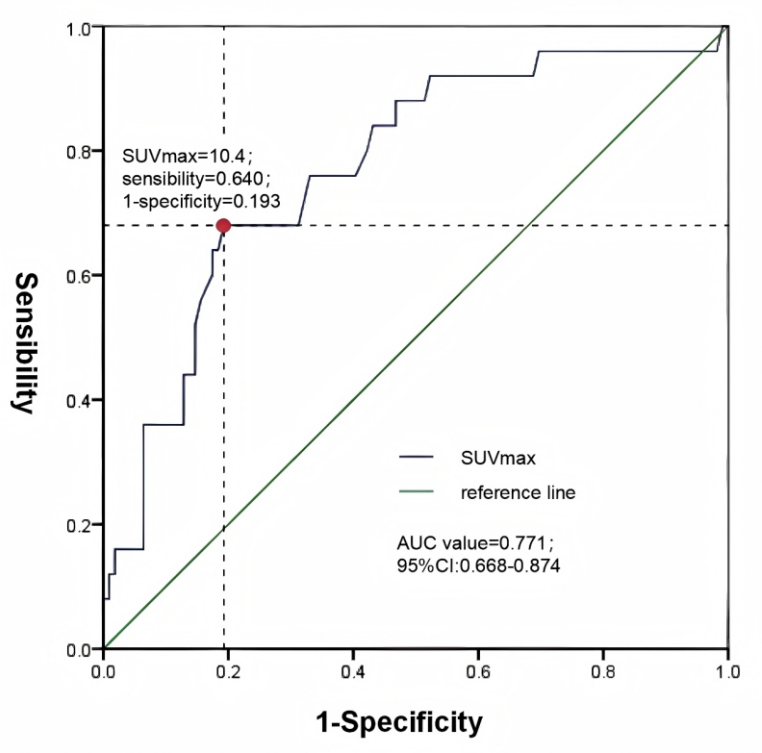

Figure 1. ROC curve for SUVmax in differentiating the cellular morphological variants of MCL.

information of tumor cells, indirectly indicating the proliferation activity and malignancy [21]. In this study, both intranodal and extra-nodal lesions of MCL showed high affinity for ^{18}F-FDG, with detection rates of 97.8% and 88.8%, respectively. However, despite ^{18}F-FDG PET/CT's high sensitivity in detecting MCL lesions, its accuracy in diagnosing various sites is controversial due to its non-specificity as a tumor imaging agent.

In our study, we compared the differences in SUVmax between pathologically confirmed lesions and positive lesions through ^{18}F-FDG PET/CT in lymph node, Waldeyer's ring, bone marrow, stomach and intestine. The results indicated that there was no statistically significant difference in lymph node, Waldeyer's ring, stomach and intestine. It showed a good consistency. However, in bone marrow, the SUVmax of the lesions identified as positive by ^{18}F-FDG PET/CT was higher than the SUVmax of pathologically confirmed bone marrow infiltration, indicating that the SUVmax of patients with MCL bone marrow infiltration may not be high.

Compared with bone marrow biopsy, ^{18}F-FDG PET/CT had good specificity and PPV in the diagnosis of MCL bone marrow infiltration (86.4% and 86.2%, respectively), but the sensitivity and NPV were not satisfactory (43.9% and 61.4%, respectively), and the diagnostic accuracy was 67.9%. This is similar to other aggressive lymphomas [22]. It suggests that when ^{18}F-FDG PET/CT reveals positive findings in the bone marrow of MCL patients, bone marrow infiltration should be strongly considered, whereas negative results do not conclusively rule out the possibility of bone marrow infiltration. Morgan et al. (2018) [23] compared multiple semi-quantitative methods and results showed that >38% bone marrow voxel had the best diagnostic ability to determine MCL bone marrow invasion (with sensitivity of 100%, specificity of 87.5%). However, there were only 11 MCL patients in this study as a development sample, and its practical application value needs to be further verified. Mayerhoefer et al. (2020) [24] indicated that radiomics can extract more imaging information and significantly enhance the diagnostic capability of ^{18}F-FDG PET/CT in bone marrow infiltration. This study offers a novel approach in this field.

The gastrointestinal tract is a common extranodal involvement site for MCL, affecting approximately 15%-30% of MCL patients [25]. In previous studies, there have been controversy regarding the use of ^{18}F-FDG PET/CT in evaluating gastrointestinal involvement in MCL, with significant variations in the results, showing a sensitivity ranging from 11% to 81% [10, 26, 27]. Skrypets et al. (2021) [27] retrospectively analyzed of 79 MCL patients. Their results indicated that the sensitivity, specificity, and accuracy of ^{18}F-FDG PET/CT in the upper gastrointestinal (GI) tract were 61.54%, 74.36%, and 71.15%, respectively. For the intestine, the corresponding values were 81.82%, 85%, and 83.87%. In our study, the diagnostic accuracy of ^{18}F-FDG PET/CT for MCL infiltration in the stomach and intestine was 85.0% and 91.7%, respectively, indicating a high diagnostic efficiency. Given the relatively small sample size and the retrospective research of this portion of the study, there exists an inherent and unavoidable risk of selection bias. It is important to note that factors such as diabetes, inflammation, and physiological uptake can all interfere with the diagnostic process [28].

We analyzed various clinical and PET/CT imaging information of MCL patients. The Ki-67 index and SUVmax showed

statistically significant differences in distinguishing between the classical and aggressive variants of MCL. Specifically, both the Ki-67 index and SUVmax were significantly higher in patients with the aggressive variant compared to those with the classical variant. Furthermore, there was a significant positive correlation between the Ki-67 index and SUVmax. When applying a SUVmax threshold of 10.4 for diagnosis, it effectively differentiated between the two pathological subtypes. As we all know, SUVmax is a semi-quantitative parameter reflecting the degree of tumor uptake of ^{18}F-FDG, while Ki-67 is a nuclear proliferation antigen that can determine the proliferation activity of tumor cells. Both SUVmax and Ki-67 index can reflect the malignancy and prognosis of tumors [29]. Our research findings not only demonstrate that SUVmax can effectively distinguish between different cytomorphological subtypes of MCL, but also possess theoretical value in indicating the prognosis and aggressiveness of the disease.

Patients with MCL often present with widespread lesions throughout the body at the time of initial diagnosis, making it clinically challenging to perform biopsies on all lesions. Due to the high heterogeneity of MCL, the aggressiveness, cytomorphological subtype, and even pathological type of lesions in different locations within the same patient may vary [30]. Additionally, some lymphomas have the potential for histological transformation [31]. Fluorine-18-FDG PET/CT can non-invasively detect lesions throughout the body. For lesions with SUVmax >10.4, there is a high likelihood of aggressive disease, which can provide clinical guidance in identifying and targeting biopsy locations. This information will assist clinicians in selecting appropriate treatment options.

In conclusion, ^{18}F-FDG PET/CT exhibits high diagnostic value for mantle cell lymphoma (MCL), and it can also utilize the SUVmax value to differentiate the cytomorphological subtypes of MCL, providing certain indications for prognosis and aggressiveness. This can serve as a reference for clinical staging and the selection of biopsy sites. However, this study has certain limitations. Firstly, it is a retrospective study with a small sample size, which inevitably introduces some selection bias. Secondly, not all abnormal lesions underwent pathological biopsy, and the diagnosis of some positive lesions relied on the experience and judgment of nuclear medicine physicians, introducing a degree of subjectivity.

Funding Wuxi Xinwu District Xinrui Hospital Scientific Research Project (2024YJYB004)

The authors declare that they have no conflicts of interest

Bibliography

1. Armitage JO, Longo DL. Mantle-Cell Lymphoma. *N Engl J Med* 2022; 386: 2495-506.
2. Hematology Oncology Committee of China Anti-Cancer Association, The Society of Hematology at Chinese Medical Association, Union for China Lymphoma Investigator at Chinese Society of Clinical Oncology. The guideline of the diagnosis and treatment of mantle cell lymphoma in China (2022). *Chin J Hematol* 2022; 43: 529-36.
3. Monga N, Tam C, Garside J et al. Clinical efficacy and safety of first-line treatments in patients with mantle cell lymphoma: A systematic literature review. *Crit Rev Oncol Hematol* 2021; 158: 103212.
4. Wu M, Li Y, Huang H et al. Initial Treatment Patterns and Survival Outcomes of Mantle Cell Lymphoma Patients Managed at Chinese Academic Centers in the Rituximab Era: A Real-World Study. *Front Oncol* 2021; 11: 770988.
5. Wang J, Zeng Q. Direct comparison of bone marrow biopsy and PET/CT for the detection of bone marrow infiltration in patients with non-Hodgkin lymphoma: a meta-analysis. *Q J Nucl Med Mol Imaging* 2024; 68(3): 161-8.
6. Dreyling M, Klapper W, Rule S. Blastoid and pleomorphic mantle cell lymphoma: still a diagnostic and therapeutic challenge. *Blood* 2018; 132: 2722-9.
7. Gerson JN, Handorf E, Villa D et al. Outcomes of patients with blastoid and pleomorphic variant mantle cell lymphoma. *Blood Adv* 2023; 7: 7393-401.
8. Le Gouill S, Długosz-Danecka M, Rule S et al. Final results and overall survival data from a phase II study of acalabrutinib monotherapy in patients with relapsed/refractory mantle cell lymphoma, including those with poor prognostic factors. *Haematologica* 2024; 109: 343-50.
9. Zanoni L, Bezzi D, Nanni C et al. PET/CT in Non-Hodgkin Lymphoma: An Update. Semin Nucl Med 2023; 53: 320-51.
10. Albano D, Ferro P, Bosio G et al. Diagnostic and Clinical Impact of Staging ^{18}F-FDG PET/CT in Mantle-Cell Lymphoma: A Two-Center Experience. *Clin Lymphoma Myeloma Leuk* 2019; 19: e457-e464.
11. Albano D, Treglia G, Gazzilli M et al. ^{18}F-FDG PET or PET/CT in Mantle Cell Lymphoma. *Clin Lymphoma Myeloma Leuk* 2020; 20: 422-30.
13. Frantellizzi V, Kovalchuk S, Linguanti F et al. Young Italian Association of Nuclear Medicine. The Role of ^{18}F-FDG PET/CT in Staging and Prognostication of Mantle Cell Lymphoma: An Italian Multicentric Study. *Cancers (Basel)* 2019; 60: 1831.
14. Johnson SA, Kumar A, Matasar MJ et al. Imaging for Staging and Response Assessment in Lymphoma. *Radiology* 2015; 276: 323-38.
15. Albano D, Bianchetti N, Talin A et al. Prognostic Role of Pretreatment Tumor Burden and Dissemination Features From 2-^{18}F-FDG PET/CT in Advanced Mantle Cell Lymphoma. *Hematol Oncol* 2025; 43: e70009.
16. Yang S, Fu L, AbuduRxiti M et al. Application of ^{18}F-fluorodeoxyglucose positron emission tomography/computerized tomography in mantle cell lymphoma. *Nucl Med Commun* 2020; 41: 477-484.
17. Swerdlow SH, Campo E, Pileri SA et al. The 2016 revision of the World Health Organization classification of lymphoid neoplasms. *Blood* 2016; 127: 2375-90.
18. Lambert L, Burgetova A, Trneny M et al. The diagnostic performance of whole-body MRI in the staging of lymphomas in adult patients compared to PET/CT and enhanced reference standard-systematic review and meta-analysis. *Quant Imaging Med Surg* 2022; 12: 1558-70.
19. Cheson BD, Fisher RI, Barrington SF, et al. Recommendations for initial evaluation, staging, and response assessment of Hodgkin and non-Hodgkin lymphoma: the Lugano classification. *J Clin Oncol* 2014; 32: 3059-68.
20. Cheson BD, Pfistner B, Juweid ME, et al. Revised response criteria for malignant lymphoma. *J Clin Oncol* 2007; 25: 579-586.
21. Ju SH, Lee SE, Yi S et al. Transcriptomic characteristics according to tumor size and SUVmax in papillary thyroid cancer patients. *Sci Rep* 2024; 14: 11005.
22. Cabezas-Quintario MA, Gomez P, Yuste-Del Pozo V et al. Bone marrow trephine biopsy involvement by lymphoma: pattern of involvement and concordance with flow cytometry, in 10 years from a single institution. *Clin Transl Oncol* 2016; 18: 537-40.
23. Morgan R, Perry M, Kwak J et al. Positron Emission Tomography-based Analysis Can Accurately Predict Bone Marrow Involvement With Mantle Cell Lymphoma. Clin Lymphoma Myeloma Leuk 2018; 18: 731-736.
24. Mayerhoefer ME, Riedl CC, Kumar A et al. ^{18}F-FDG-PET/CT Radiomics for Prediction of Bone Marrow Involvement in Mantle Cell Lymphoma: A Retrospective Study in 97 Patients. *Cancers (Basel)* 2020; 12: 1138.
25. Oña-Ortiz FM, Sánchez-Del Monte J, Ramírez-Solís ME et al. Mantle cell lymphoma with involvement of the digestive tract. Linfoma del manto con afección del tubo digestivo. *Rev Gastroenterol Mex (Engl Ed)* 2019; 84: 434-41.
26. Hosein PI, Pastorini VH, Paes FM et al. Utility of positron emission tomography scans in mantle cell lymphoma. *Am J Hematol* 2011; 86: 841-5.

27. Skrypets T, Ferrari C, Nassi L et al. ^{18}F-FDG PET/CT Cannot Substitute Endoscopy in the Staging of Gastrointestinal Involvement in Mantle Cell Lymphoma. A Retrospective Multi-Center Cohort Analysis. *J Pers Med* 2021; 11: 123.
28. Lovinfosse P, Hustinx R. The role of PET imaging in inflammatory bowel diseases: state-of-the-art review. *Q J Nucl Med Mol Imaging* 2022; 66: 206-17.
29. Li H, Wang X, Zhang L et al. Correlations between maximum standardized uptake value measured via ^{18}F-fluorodeoxyglucose positron emission tomography/computed tomography and clinical variables and biochemical indicators in adult lymphoma. *J Cancer Res Ther* 2019; 15: 1581-8.
30. Nishioka A, Ureshino H, Ando T et al. Three coexisting lymphomas in a single patient: composite lymphoma derived from a common germinal center B-cell precursor and unrelated discordant lymphoma. *Int J Hematol* 2018; 107: 703-8.
31. Parry EM, Roulland S, Okosun J. DLBCL arising from indolent lymphomas: How are they different? *Semin Hematol* 2023; 60: 277-84.